

Static Contact Simulation Analysis of Belt Grinding on Blade Surface

Hongbin Lv, Yuefeng Wu, Jifa Cheng, Wengang Fan*

School of Mechanical, Electronic and Control Engineering, Beijing Jiaotong University, Beijing 100044, China

*Corresponding Author

Keywords: Belt grinding; blade surface; contact; finite element simulation

Abstract: The static contact behavior of CNC abrasive belt grinding on a blade surface was determined through the finite element method. The characteristics of the blade surface were extracted, and the static contact finite element simulation models of real blade surface, parametric surface, and special surface were established. By analyzing changes in contact stress, contact area, shape of contact area, displacement of the contact surface, and other parameters, the relationship between contact status and workpiece surface curvature on CNC abrasive belt grinding of blade surface was revealed. The best processing quality was obtained when the curvature direction of the contact wheel matches the minimum principal curvature of the target point, and the stress along each direction was positively correlated with the curvature in that direction. This result provides a basis for the design and posture control of contact wheel on the CNC abrasive belt grinding of a blade surface.

1. Introduction

Complex blades are the key structural components of energy conversion devices, such as steam turbines, aero engines, and ship propellers. Harsh working conditions impose stringent requirements on blade materials and manufacturing quality and efficiency [1]. Blades are usually made of difficult-to-machine materials and have complex profiles; thus, blade processing accounts for nearly one-third of the total equipment manufacturing workload [2]. At present, blades are generally processed after near net forming, and abrasive belt grinding is an important part of the process; its feasibility has been fully verified [3]. Abrasive belt grinding is known as “cold grinding,” and its unique elastic characteristics make it highly flexible and adaptable [4]. RECH et al. studied the abrasive grinding of hardened steel material and pointed out that belt grinding not only can create compressive stress on the surface of the workpiece but also can greatly improve surface roughness [5]. CNC belt grinding is considered the best method for blade profile processing [6].

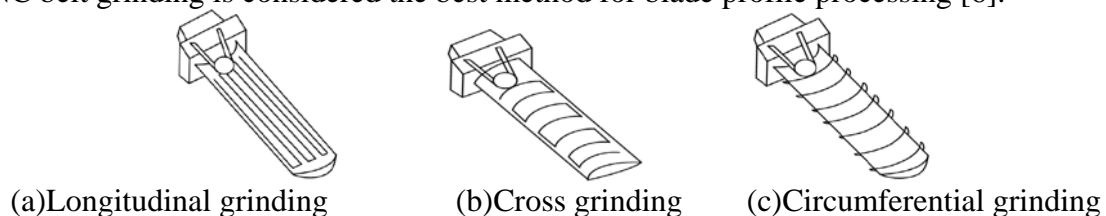


Fig.1 Different forms of CNC belt grinding for blade-like surfaces

Given the shape and complexity of blade and the flexibility of a contact wheel, the shape of a material removed by a single pass has the characteristics of “following shape,” which makes the precise control of material removal during belt grinding difficult [7]. Most existing systems use the parameter line method or the equal section method to process them directly. In these methods, the direction of the path and the initial tool path are determined first, but machining accuracy cannot be effectively guaranteed along the processing path because of the varied shapes of the complex surface geometry [8]. In this paper, the contact simulation process in the grinding of the blade-type surface of the abrasive belt was investigated, and the complex nonlinear mechanism of the elastic grinding process was comprehensively examined. The influence of the curvature change during the

contact process was deeply analyzed. Our findings provide basis and support for solving the problem of precision grinding of CNC belts in domestic blade-like surfaces.

2. Contact simulation of real blade grinding process

2.1 Contact simulation of real blade grinding process

Contact state during the processing of the existing blade is simulated. A type of aero engine blade is selected as the research object, and the model is simplified. Plastic deformation is small because no relative sliding occurs between the contact wheel and the abrasive belt in the actual processing and the thickness of the abrasive belt substrate is only 0.1–0.3 mm, which is much smaller than the radius of the contact wheel. Therefore, the contact wheel and the belt are considered one body during the modeling, and the thickness of the belt is ignored. In the aeronautical blade grinding process, the contact wheel is in an elastic contact state at the contact between the contact wheel and workpiece, and the local total plastic deformation does not exceed one percent of the contact wheel radius because the amount of material removed is small. Thus, the model can be simplified as contact between the contact wheel and surface of the workpiece, the contact wheel is subjected to positive pressure, and the surface of the workpiece is a rigid surface. Aluminum core and workpiece using C3D8R element, rubber layer due to its special high elastic characteristics, using C3D8RH element, the blade surface due to its complex curvature changes, using C3D10M element. To improve calculation accuracy and calculation efficiency, the mesh is refined in the contact area, whereas the aluminum core adopts a thicker mesh, and the rubber layer and the aluminum core mesh are coupled by coupling, specific material parameters, and selected element types, as shown in Table 1.

Table 1 Properties of workpieces and grinder

Properties	Core	Blade	Rubber
Density (kg/m ³)	3960	8240	1000
Elastic Modulus (Mpa)	3.7e5	2.04e5	7.84
Poisson ratio	0.22	0.3	0.49
Element type	C3D8R	C3D10M	C3D8RH

The surface continuity of the real blade surface is analyzed by using the zebra pattern test. The analysis results show that the surface of the blade is at least second-order continuous. Five different machining positions are selected for finite element analysis(**Fig.2**). We set the grinding pressure to 15 N and ensure that the contact wheel is positioned on the trajectory and is tangent to the blade surface.

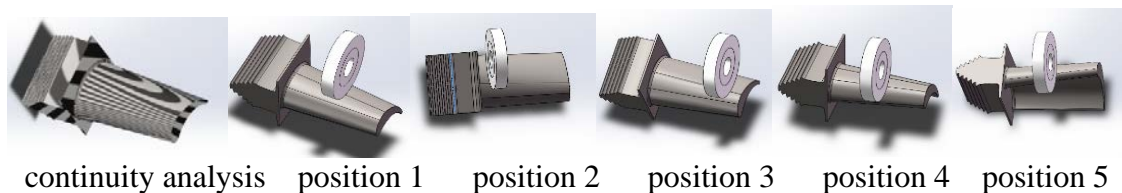


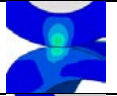
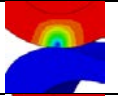
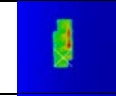
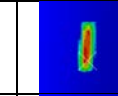
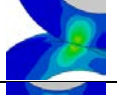
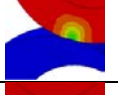
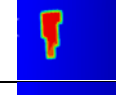
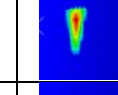
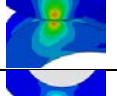
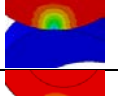
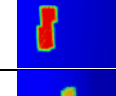
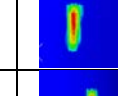
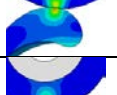
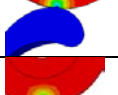
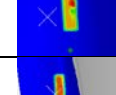

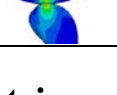

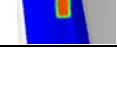

Fig.2 Different machining positions and continuity analysis of blade surface

2.2 Result analysis

The displacement, stress, contact area, and contact pressure were extracted in the real blade simulation model, as shown in Table 2. Analysis of the simulation results shows that when the contact wheel is in different positions in actual blade grinding, the local curvature of the blade affects the stress and strain values under the same parameters, and the actual contact area and shape and the contact pressure vary greatly and have no obvious regularities. The maximum stress varies from 3 Pa to 9 Pa. The maximum displacement of the contact wheel at the contact point is 3.2–4.8 mm, and the fluctuation amplitude exceeds 50%. The displacement of the blade surface is nearly zero compared with the contact wheel; that is, deformation is negligible. Thus, treating the surface

of a workpiece as a rigid surface is appropriate. The contact areas vary in shape, and the maximum contact pressure varies from 7.3 N to 9.2 N. These results indicate that controlling the processing quality of a contact wheel by adjusting the position and pose of contact wheel in constant pressure belt grinding is difficult when the influence of surface curvature is not considered and the gap is obvious.

Table 2 Contour of blade surface

Position	S,Mises	U	CNAREA	CPRESS
Position 1				
Position 2				
Position 3				
Position 4				
Position 5				

3. Contact simulation of parametric surface

3.1 Modeling and Analysis of Parametric Surfaces

To study the influence of the curvature characteristics of the contact points on the internal stress and contact state of the workpiece after machining, a parametric surface based on the true curvature and thin wall features of the blade was established. Its surface equation is

$$\begin{cases} x = -94.4 + 88.9v + 5.6v^2 \\ y = -131.u + 28.1u^2 \\ z = 5.9(u^2v^2 + u^2v) - 3.9uv^2 + 76.2u^2 + 6.7v^2 - 27.3uv - 50.8u + 25v + 12.1 \end{cases} \quad (1)$$

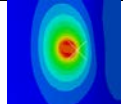
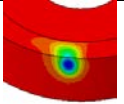
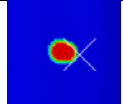
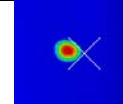
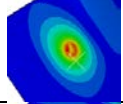
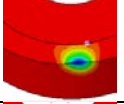
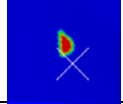
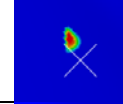
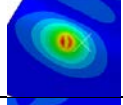
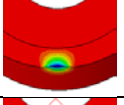
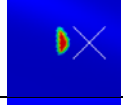
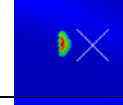
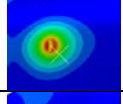
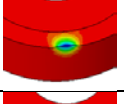
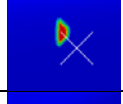
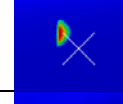
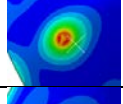
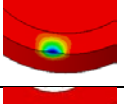
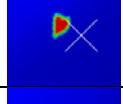
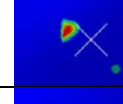
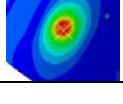
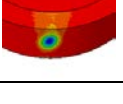
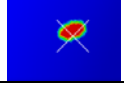
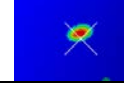
The surface parameters are jointly modeled by Matlab and Solidworks, and point with parameter value of 0.5 for u and v is obtained during simulation. After analyzing the local curvature feature, we found that the point is an elliptic point. The continuity analysis and Gaussian curvature analysis of the surface show that the surface is at least second-order continuous. Other degrees of freedom are limited and leave only the rotational freedom of the contact wheel around the tool axis as a single variable, which can also be described as the angle between the maximum normal direction of the workpiece contact point and the axis of the contact wheel. Owing to the symmetry of the contact wheel itself and the asymmetry of the curvature of the target surface, the change of each contact parameter under different angle states is analyzed from 0° to 180° every 30° .

3.2 Result analysis

When the angle between the maximum normal direction and the axial direction of the contact wheel changes, stress, deformation, and contact state vary. The smallest workpiece stress, most deformed rubber layer, and largest contact area are observed at an angle near 0° . Moreover, the shape of the contact area changes, and the smallest distance between the contact area and the ellipse and the smallest contact pressure are observed. The indicators in all other directions share no obvious relationship with change in angle, and no regularity occurs because of the different curvatures of the points in each direction. In most cases, the edge of the contact wheel first touches the surface of the workpiece instead of the midpoint of wheel; that is, the stress center point and the

target contact point do not coincide, and no effective fit is formed [9]. The best fit is obtained near 0° . When selecting the parameters of the contact wheel, curvature interference between the contact wheel and the workpiece surface should be avoided, and appropriate contact wheel shape and width should be selected.

Table 3 Contour of parameter surface

Angle	S,Mises	U	CNAREA	CPRESS
0°				
30°				
60°				
90°				
120°				
150°				

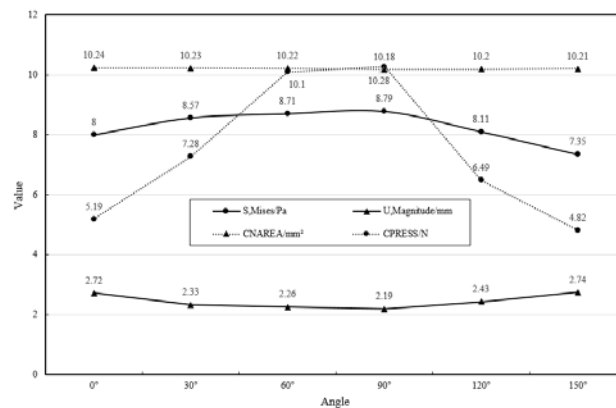


Fig.3 Data analysis of parametric surface simulation

4. Contact simulation of special surface

4.1 Classification and modeling of special surface

The blade-like surface is a typical free-form surface. The contact state during the machining process is related to the local characteristics of the contact point in addition to the curvature characteristics of the contact point. Therefore, the contact simulation analysis of the special surface is required.

Gaussian curvature and mean curvature are the inherent properties of a surface. After the surface is arbitrarily rotated, no change in the Gaussian curvature H and average curvature K of the surface is observed. This finding thereby provides a reliable guarantee for the analysis of the shape of a point on the analysis surface and its domain. The limit curvature $\{k_{\max}, k_{\min}\}$ and curvature $\{H, K\}$ has the same effect on surface information. These intrinsic curvature properties of surfaces are the basis for surface segmentation. The geometric parameters, Gaussian curvature, mean curvature,

principal curvature, and so on at each discrete point are calculated, and then the shape of the local region near the discrete point is divided into three main characteristic surface shapes, namely, elliptical surface, hyperboloid, and paraboloid by the value of the geometric parameter.

Table 4 Classification of points

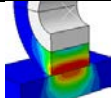
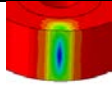
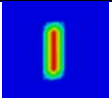
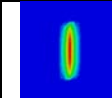
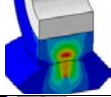
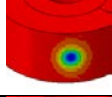
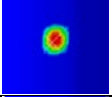
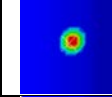
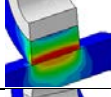
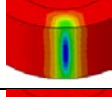
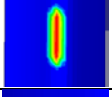
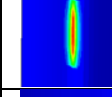
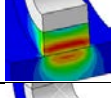
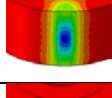
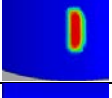
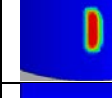
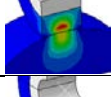
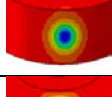
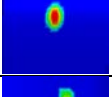
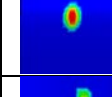
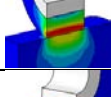
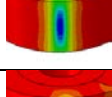
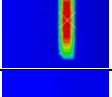
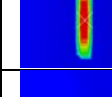
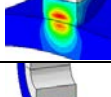
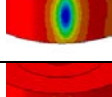
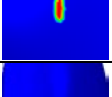
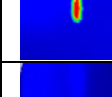
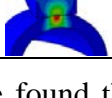
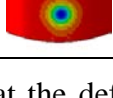
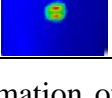
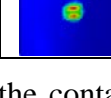
	$K>0$	$K=0$	$K<0$
$H>0$	Concave Elliptical	Concave Paraboloid	Hyperboloid
$H<0$		flat	Hyperboloid
$H=0$	Convex Elliptical	Convex Paraboloid	Hyperboloid

The nature of a point is determined by the difference of the Gaussian curvature symbol; thus, the boundary point can be obtained based on the change of the Gaussian curvature symbol; that is, a certain spatial point must be used as the adjacent surface between two adjacent Gaussian curvature change points. The boundary point between the classes is obtained from the intersection points of the adjacent two points and the vertical bisector [10].

For different special surfaces, a plane, a curved surface with a single bending direction, a hyperboloid surface, and an elliptical surface are selected for comparative simulation analysis. The radius of the unidirectional curved surfaces are 50 and 100 mm, respectively. The curvature direction and the axial direction of the contact wheel use the orthogonal and parallel states; the hyperboloid face is $a=b=100$, and the ellipse face is $a=50$, $b=100$, $c=50$.

4.2 Result analysis

Table 5 Contour of special surface

Surface type	S,Mises	U	CNAREA	CPRESS
flat				
R 50 Angel 90°				
R 50 Angel 0°				
R 100 Concave surface				
R 100 Angel 90°				
R 100 Angel 0°				
Hyperboloid surface				
Elliptical surface				

By analyzing the simulation data, we found that the deformation of the contact wheel in each direction of curvature is positively correlated with the curvature of the direction and the stress distribution is the same. By comparing the unidirectional convex surfaces with the radius of curvature of 50 and 100 mm in the orthogonal mode, we found that the maximum stress of the former is 25% larger than that of the latter, and the situation is the same in the parallel mode. This result shows that the flatter the surface, the smaller the stress. The stress values in all convex

contacts are smaller than the planar contact, and the plane can be considered a convex surface with an infinite radius of curvature. The stress on the concave surface decreases because the curvature direction of the concave surface is opposite to the curvature direction of the contact wheel; thus, the fit between the outer surface of the contact wheel and the target surface improves, and the hyperboloid surface and the elliptical surface have the same trend in each direction. After the extraction of the displacement and actual contact area of the rubber layer of contact wheel, the contact portion forms an elliptical region, and the length of the long and short axis projected by the elliptic region is related to the curvature direction and curvature radius of the two contact surfaces in all orthogonal contact modes. In the parallel contact mode, when the curvature direction of workpiece surface and the curvature direction of contact wheel surface are identical, the contact area is approximately a rectangle, and obvious stress concentration occurs on the middle line. This concentration is caused by the extrusion deformation of rubber layer under stress. The contact pressure, stress, and displacement distribution of the contact wheel are consistent.

Table 6 Data of special surface

Surface type	flat	R 50 Angel 90°	R 50 Angel 0°	R 100 Concave	R 100 Angel 90°	R 100 Angel 0°	Hyperboloid	Elliptical
CNAREA /mm ²	452.9	163.5	306.8	221.3	338.1	480.3	316.5	169.9
CPRESS /MPa	0.3249	0.8263	0.493	0.6527	0.3349	0.3042	0.5087	0.9336

5. Contact simulation of special surface

(1) For real blade surfaces, the contact state and stress distribution greatly vary at different processing positions owing to the complex and irregular curvature of the profile.

(2) By analyzing the surface simulation data of specific parameters surface, we found that the smallest stress, the best matching state of the contact surface, and the highest surface processing quality are obtained when the contact wheel and the minimum principal curvature of the target surface are matched.

(3) Contrast analysis between special curved surfaces shows that the relationships among contact pressure, stress, contact wheel displacement, and the local state and curvature of the curved surface are determined. The stress value in each direction is proportional to the curvature of the direction. Contact state is enhanced and stress is decreased when surface flatness is improved.

References

- [1] J. F. G. Oliveira, E. J. Silva, C. Guo, F. Hashimoto. Industrial challenges in grinding[J]. Manufacturing Technology, 2009, Volume 58, Issue 2: 663~680.
- [2] Chen Yanjun. Research of grinding capability of coated abrasive belt in grinding the material of gas turbine blades [D]. Chongqing University, 2006.
- [3] Zhang Yue. Machining method and key technology research on auto-programming of aircraft blade seven axis nc abrasive belt grinding [D]. Chongqing University, 2012
- [4] Huang Yun, Huang Zhi. Modern abrasive belt grinding technology and engineering application [M]. Chongqing: Chongqing University Press, 2009.
- [5] RECH J, KERMOUCHE G, GRZESIK W, et al. Characterization and modelling of the residual stresses induced by belt finishing on a AISI52100 hardened steel[J]. Journal of Materials Processing Technology, 2008, 208(1-3): 187-195.
- [6] Zhao Bomin, Zhao Bo. Modern grinding technology [M]. Beijing: China Machine press, 2003.
- [7] Wang Yajie. Precision abrasive belt grinding research based on contact theory [D]. Chongqing University, 2015.
- [8] Liu Feipeng. Research on five-axis CNC tool path planning based on the slice with mean curvature matching [D]. Guangdong University of Technology, 2011.
- [9] Lin Xiaojun, Yang Yan, Wuguang, et al. Five-axis linkage flexible cnc abrasive belt polishing technology for blade profile [J]. Journal of Aeronautics, 2015(06): 2074-2082.

[10] Wu Pengcheng. Research on ball cutters nc machining tool path planning based on the surface subdivision [D]. Nanchang University, 2012.